Construction and Building Materials 24 (2010) 918–926

Contents lists available at ScienceDirect

Construction and Building Materials

journal homepage: www.elsevier.com/locate/conbuildmat

A new bonded vertical joint design for architectural panels

G. Barluenga [a,*], F. Hernández-Olivares [b], B. Parga-Landa [c], M.J. Cowling [d]

[a] Departamento de Arquitectura, Escuela Técnica Superior de Arquitectura y Geodesia, Universidad de Alcalá, C. Santa Úrsula, 8, Alcalá de Henares-28801, Madrid, Spain
[b] Departamento de Construcción y Tecnología Arquitectónicas, Escuela Técnica Superior de Arquitectura, Universidad Politécnica de Madrid, Avda. Juan de Herrera, 4, 28040 Madrid, Spain
[c] Departamento de Arquitectura y Construcciones Navales, Escuela Técnica Superior de Ingenieros Navales, Universidad Politécnica de Madrid, Avda. Arco de la Victoria s/n, 28040 Madrid, Spain
[d] Glasgow Marine Technology Centre, James Watt Building, University of Glasgow, Glasgow G12 8QQ, UK

ARTICLE INFO

Article history:
Received 13 October 2008
Received in revised form 19 November 2009
Accepted 25 November 2009
Available online 28 December 2009

Keywords:
Steel architectural panels
Vertical joint
Toughened epoxy resin
Temperature
Thickness
Mechanical properties

ABSTRACT

This paper presents a new bonded vertical joint design for façade architectural panels which improves the façade behaviour under static and dynamic loads and enhances durability. Furthermore, it overcomes more of the structural, construction and aesthetic problems that could appear on precast façade panels. This study reports the current problems of steel façade panels and the advantages achieved with the new vertical joint design, bonded with a toughened epoxy resin. The experimental study of the new joint behaviour includes mechanical standard tests on the adhesive behaviour and non-standard static and dynamic tests performed on half scale mild steel specimens bonded with the toughened epoxy resin in order to determine its mechanical behaviour under external loads. The experimental results can be useful to calibrate numerical models of the new joint behaviour.

© 2009 Elsevier Ltd. All rights reserved.

1. Introduction

The use of façade prefabricated panels with cast-in-place joints are one of the most developed solutions for building applications. The panels can be made of mould shaped materials (i.e. lightweight or reinforced concrete) or conformed materials (i.e. metallic sandwich panels). The joints are usually made of polymeric materials, such as silicones or neoprene [1], which combine a high strain capacity and sealant ability.

Compared with casting-in-place, prefabrication offers great advantages: factory conditions improve quality control; the manufactured component is superior in accuracy, strength and weathering; and on-site time is drastically reduced. However, these systems had introduced aesthetic limitations derived from the repetition of shapes and the fixed joint dimension. They also need technical means for its proper execution at the building place and limit placement tolerances.

From a structural point of view, new problems arise concerning to the durability of the joint materials and their limited capacity to take up small displacements to adapt the drift of the main structure [2]. These problems reduce the use of prefabricated systems in situations of exposure to horizontal dynamic forces, such as wind and seismic loads [3].

The behaviour observed on load-bearing prefabricated concrete façade panels and a literature review lead to design and develop a new vertical joint for façade panels [4,5]. Fig. 1 shows the horizontal section of the new design and a perspective view. The novelty of the design is the inclusion of a V-shaped joint piece, made of similar materials than the prefabricated panels, that fits inside the V-shaped joint gap left between two adjacent panels and an adhesive joint material.

In the construction process, the joint is cast-in-place after the prefabricated architectural panels have been placed at the building site, as it is shown in Fig. 2. The adhesive joint material is placed on both surfaces of the panels to bond the joint piece to the panels.

Fig. 3 present the external loads that apply on cladding joints, in-plane and transversal (perpendicular-to-plane) actions have to be taken into account [4,5].

The main goals achieved by this new joint design are:

- From a *structural* point of view, this configuration makes the joint tougher and more durable. The conventional prefabricated systems have straight joints, perpendicular to the façade plane. When the cracks that can appear in the joint reach a critical size they propagate mainly under tensile stresses (fracture mechanic mode I). After this V-joint design the cracks have to propagate by

* Corresponding author. Tel.: +34 91 883 92 39; fax: +34 91 883 92 76.
E-mail address: gonzalo.barluenga@uah.es (G. Barluenga).

0950-0618/$ - see front matter © 2009 Elsevier Ltd. All rights reserved.
doi:10.1016/j.conbuildmat.2009.11.026

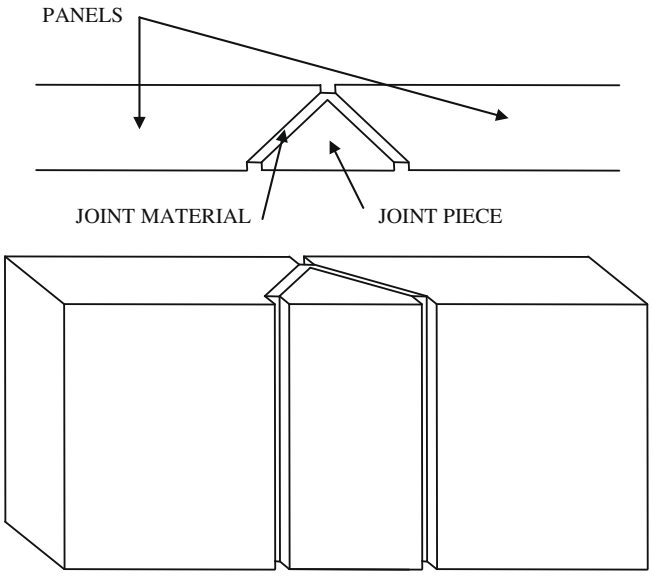

Fig. 1. New vertical joint design for architectural panels. Horizontal section.

a combination of tensile and shear stresses (fracture mechanic mixed mode I and II). The energy required by crack propagation by mixed modes I–II is always larger than that under single mode I; therefore, this new design of joint increases its toughness in fracture.

- This design reduces the debonding risks compared with conventional joints, as the adhesive layer has larger contact surface with the adherends.
- This joint configuration gives some mechanical continuity to the façade, although it keeps some deformability. The joint layout allows the collaboration of the viscoelastic damping capacity of the joint material against horizontal dynamic loads (wind and seismic loads), as it is shown in Fig. 3. With the proper joint material, this joint could become a passive damping device [3,4,6]. In conventional prefabricated systems, connections transmit panel loads and, due to this fact, cladding systems are severally penalized in seismic regulations [3].
- From a *construction* point of view (see Fig. 2), the new joint simplifies the application of the joint material. In the conventional configurations, the gap that constitutes the joint is around 2 cm width and the application of the joint material becomes difficult. In this new design, the joint piece is placed after the joint material, which allows a proper application of the joint material as the gap left is wider.
- It minimizes the incidence of local defects of the joint material that can arise due to improper application. As the joint material is distributed on a surface around 1.5 times wider than in conventional joints, the joint is waterproofing, because a local defect does not compromise physical continuity.
- It attenuates the effect of hygrothermal variations on the joint material, the erosion due to climatic actions and the ageing produced by ultraviolet radiation. The joint piece protects the joint material from direct actions and, due to its thermal inertia, absorbs peak temperatures, enlarging the durability of the physical properties and performance features of the joint material.
- Concerning *aesthetic*, this configuration allows either hiding or expressing the space of the joint, including the joint in the façade design. The exterior finishing of the joint piece can be adapted to the project needs, with different materials, colours or textures.
- As the joint configuration has significant exterior dimensions, it can become an aesthetic element (a pilaster, for example). The joint piece can be included in the façade thickness (in order to hide it) or overcome the façade external face (when the designer decides to highlight it). In conventional prefabricated façade, straight joints, aesthetically, suppose a discontinuity [2].

The advantages of this new design for vertical joint over conventional joints for prefabricated concrete architectural panels have been already described and SBR latex modified mortar showed to be an adequate joint material [5,6].

In this paper, a study on the use of this new joint on steel panels for façade, bonded with a commercial toughened epoxy resin, is described. Some half-scaled specimens of the joint were built and some tests were run in order to characterize the materials and to analyze its behaviour under static and dynamic loads. Tests were run at several temperatures and different joint thicknesses, considering environmental and dimensional variations arisen due to an improper execution, respectively.

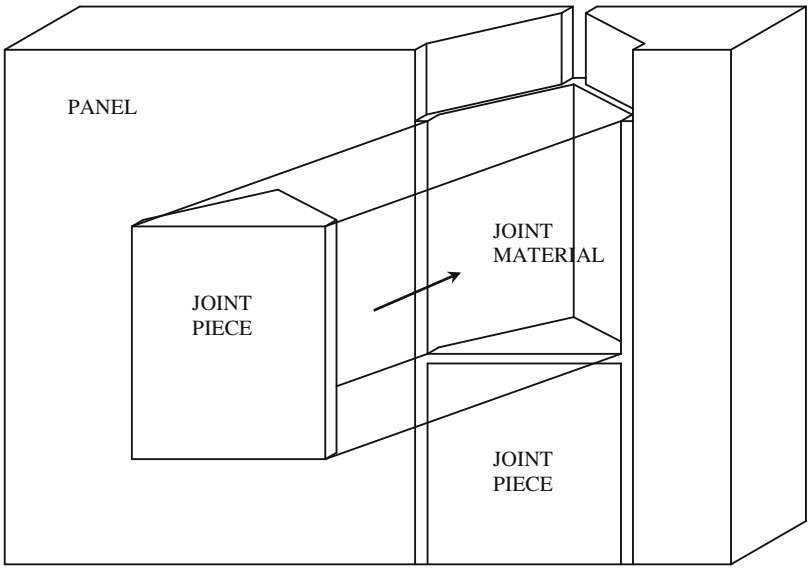

Fig. 2. Building process of the new vertical joint design for architectural panels.

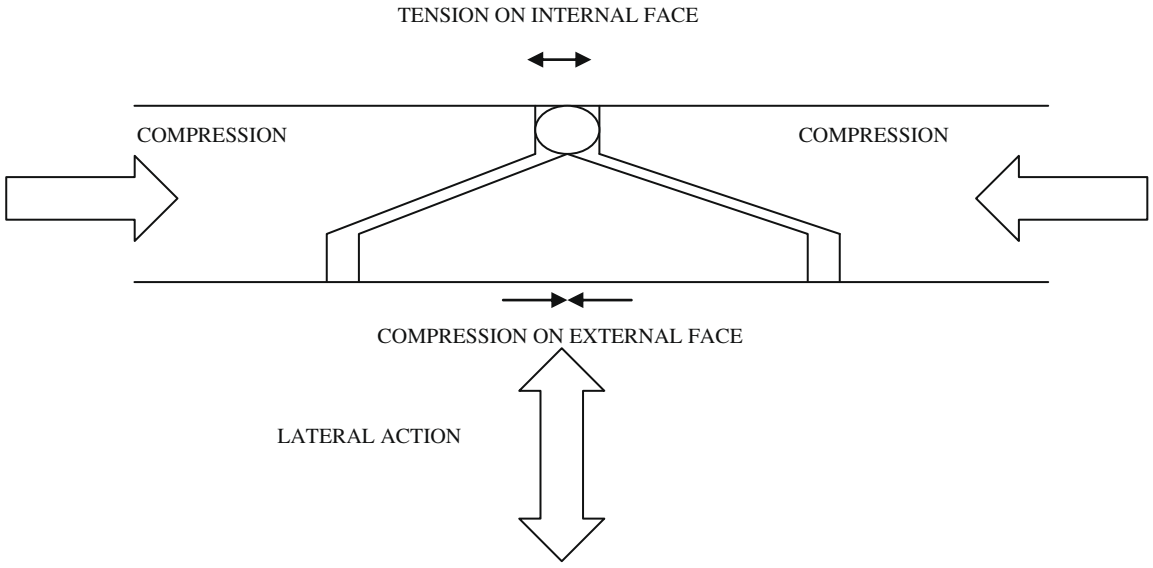

Fig. 3. Stress state at the joint due to external actions (hygrothermal, load-bearing and wind forces).

2. Material selection and bonding procedure

Adhesive jointing has been extensively used in several engineering structural applications, as marine technology [7–9]. Typically, the main properties of the adhesive required to analyse the stresses in adhesive joints are the tensile (Young) modulus, the shear modulus and the yield stresses, the fracture stresses and strains in uniaxial and in pure shear [10].

Although, in some other applications, when moderately high temperatures can be reached, some problems concerning with softening and decrease of strength have been described [11,12].

When adhesives are used in architectural applications in a Mediterranean environment, combining sun heating and humidity, it has been observed that temperatures can reach 40–50 °C that can produce an important decrease of adhesive bonding capacity [13,14].

Considering the construction process of the new vertical joint design, some basic adhesive features were defined, as low tensile modulus, high thixotropy and flexibility in a paste state and large strain before break point after hardening (toughness). Accordingly, a commercial two components toughened epoxy resin (Permabond™ E04) was selected. Its main nominal properties were full cure time in 24 h, maximum gap fill of 5 mm and shear strength of 21 MPa, at room temperature conditions [15].

A toughened epoxy can be defined as an epoxy resin (thermosetting polymer) modified in order to increase resistance to crack propagation and impact strength, without significantly decreasing other mechanical properties as modulus or thermal sensitiveness [16–19]. Toughness is often improved by introducing a dispersed rubber phase into the primary epoxy phase [17].

The purpose of toughening a material is to increase its ductility and decrease the possibility of brittle fracture [18]. It should be remembered that, as in any other thermosetting adhesive, environmental conditions have significantly effects on a toughened epoxy mechanical performance [19].

To achieve a good adhesive performance, all the specimens were hot cured at 60 °C, for 30 min after the adhesive layer reached the curing temperature [11], measured with a thermocouple located at the adhesive layer. This procedure corresponded to the reduction of curing time recommended by the producer [15]. The cooling process of the specimens was controlled, minimizing the stress concentrations at the contact surfaces due to the different thermal inertia of adhesive and adherends.

The adherends were considered rigid, since their stiffness was 200 times larger than the stiffness of the adhesive. The contact surfaces of the adherends were shotblastered to guarantee a cohesive failure. The spew fillet of adhesive was scratched to obtain a strength value as real as possible, without damaging the adhesive layer.

3. Specimen preparation and testing

In order to characterize the toughened epoxy resin, series of three shear and cleavage standard tests were performed (ASTM D 3175-73 and 1062-78, respectively). Fig. 4 illustrates the principles of both tests. Basic pure tensile tests were not considered because the joint design intentionally avoids direct tension and cleavage already combines tension and bending.

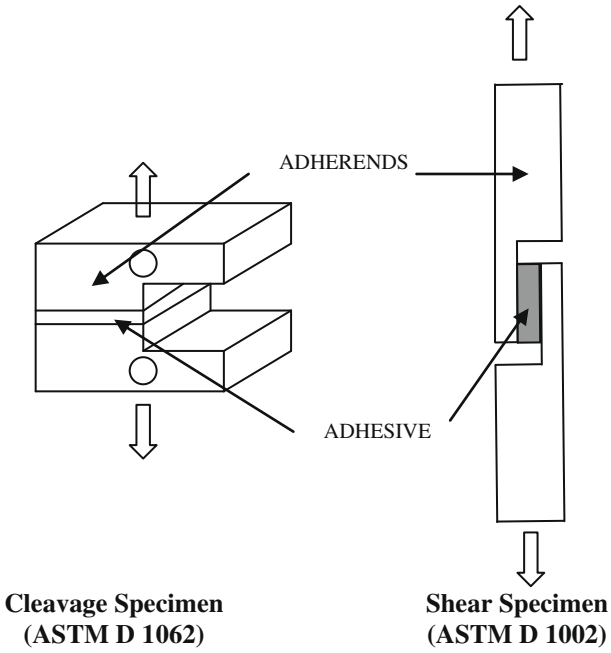

Fig. 4. Cleavage and shear standard tests principles.

Different thicknesses at several temperatures were tested. The thermal range analyzed corresponds to a template Mediterranean country (from 0 to 60 °C) [13,14]. The specimens were maintained at the testing temperature for 15 min, measured with a surface thermocouple, to guarantee that the entire adhesive layer had reached it.

To study the new bonded joint design, half scale mild specimens of the joint configuration were designed and mechanized for compression and bending tests. Specimen dimensions and designs are presented in Fig. 5.

In order to avoid buckling, the specimens had a thickness of 45 mm. The specimens under test were instrumented with linear transducers (LVDT) and the test results were recorded with a data acquisition system (Fig. 6).

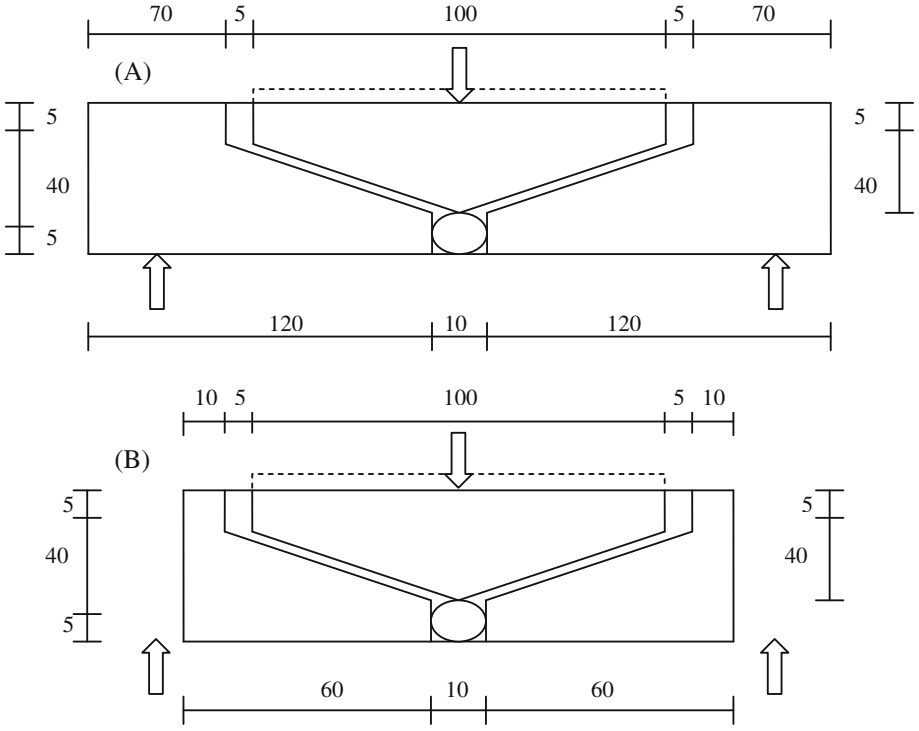

Fig. 5. Non-standard test specimen designs: (A) bending and (B) compression (dimensions are in mm. The thickness of all specimens was 45 mm.).

Bending specimens were tested in a three points bending method, with a span of 200 mm (Fig. 7). Afterwards, the adhesive layer thickness was changed in order to study its influence on the joint behaviour under static and dynamic loads. Asymmetric and symmetric configurations were tested. The asymmetric configuration trends to reproduce dimensional variations arisen due to improper joint execution.

A compression specimen under testing can be observed in Fig. 8.

4. Experimental results

Shear tests were managed in the thick-adherend standard method (ASTM D 3175-73). Sets of three specimens were tested, in order to obtain a valid statistical value. They were tested under several temperatures with different thicknesses (Table 1) to record the influence of these features on the mechanical behaviour of the bonding material.

Shear stress (τ), shear strain at maximum stress (γ), shear modulus at origin (G) and linear modulus (E) results were calculated by Eqs. (1)–(4) respectively, and the test results are recorded in Table 1:

$$\tau = \frac{P}{h \times b} = \frac{P}{25\ \text{mm} \times 15\ \text{mm}} \tag{1}$$

$$\gamma = \frac{\delta}{t} \tag{2}$$

$$G = \frac{\tau}{\gamma} = \frac{P \times t}{A \times \delta} \tag{3}$$

$$E = 2G \times (1 + \upsilon) \approx 3G \tag{4}$$

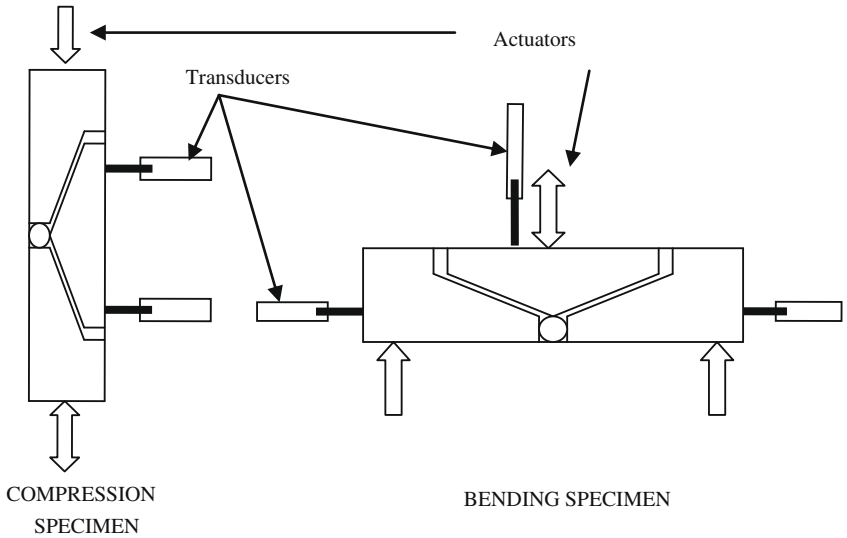

Fig. 6. Compression and bending non-standard specimens; test setup.

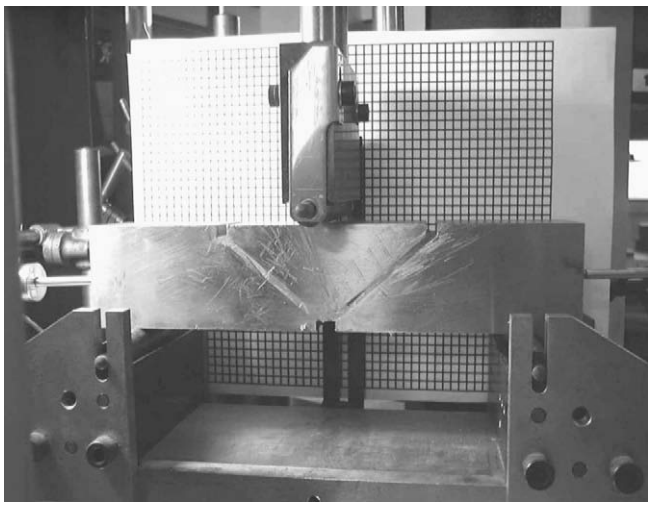

Fig. 7. Non-standard bending specimen under testing.

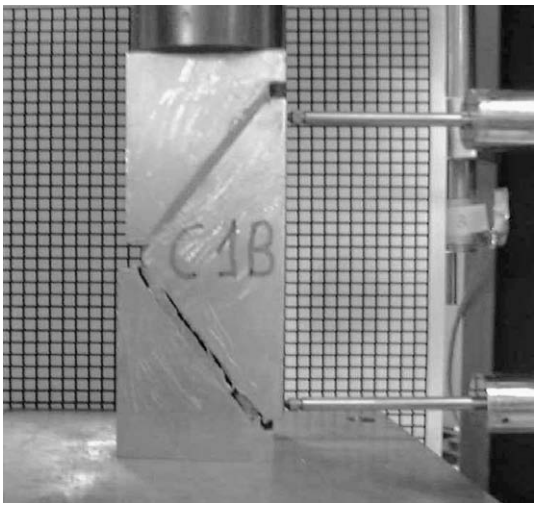

Fig. 8. Non-standard compression specimen under testing.

where P is test load, h is adhesive layer height, b is adhesive layer width, δ is maximum test displacement, t is adhesive layer thickness and υ is Poisson coefficient.

As it is shown in Fig. 9, the increase of temperature produced a dramatic decrease of shear strength. In fact, at 0 and 20 °C, the failure was cohesive, while at 60 °C debonding of the adhesive happens (interfacial failure).

Cleavage standard tests (ASTM 1062-78) were performance in sets of three specimens. Four temperatures and four thicknesses were tested (Table 2).

Average cleavage stress and maximum cleavage stress were calculated using Eqs. (5) and (6), respectively, from the standard cleavage tests and the test results obtained are recorded in Table 2:

$$\sigma_{ave} = \frac{P}{b \times h} \tag{5}$$

$$\sigma_{\max} = \frac{P}{A} + \frac{M}{W} = \frac{P}{b \times h} + \frac{P\frac{h}{2}}{\frac{b \times h^2}{6}} = \frac{4P}{b \times h} \tag{6}$$

where P is test load, h is adhesive layer height, b is adhesive layer width, A is the bonded area, M is the bending moment produced by cleavage and W is the elastic section modulus.

In this case, only the specimens with an adhesive layer thicker than 1.5 mm and at temperatures higher than 40 °C showed interfacial failure (debonding). In all the other specimens the failure was cohesive. As the thickness of the adhesive layer increased, a decrease of the cleavage strength occurred at all the temperatures tested (Fig. 10). The load–displacement graphic fits with a parabolic branch. These results accorded with the behaviour of this kind of adhesive [13].

Three point static bending tests of the new configuration were carried out in sets of three specimens at room temperature (20 °C). Three different configurations, considering different adhesive layer thicknesses, were tested (Table 3).

Two load speeds (0.5 and 1 mm/min) were used, but no difference of neither the behaviour nor the failure strength was recorded. The curve "load–displacement of the load head" showed a first stage, where there was an increase of the stiffness, and a second one characterized by its lineal shape till failure (Fig. 11a). A brittle failure happened at the lower edge of the adhesive layer.

The graphic that plots "load versus lateral displacement measurements" (Fig. 11b) shows two different behaviours: One side of the specimen showed a first stage similar than the main graphic and a second stage where the increase of load did not produce an increase of the lateral displacement. On the other side of the specimen, where the failure happened, the graphic fits with a parabolic branch (as it happened in cleavage tests).

The static compression tests of the new joint design were performed on compression specimens with a 2.5 mm symmetric adhesive layer. Two load speeds (0.5 and 1 mm/min., displacement controlled test) were used, but no difference of neither the behaviour nor the failure strength was recorded.

The curve "load–displacement of the load head" shows a bilinear behaviour before maximum strength and a slender decrease of the load level as the displacement increase (Fig. 12). The failure happened after a long deformation period.

Dynamic three point bending tests were performed on the three different configurations described for static bending tests. Two

Table 1
Shear standard test results.

Shear tests adhesive thickness (mm) and test temperature	Shear load (N)	Displacement at failure (mm)	Shear stress (MPa)	Shear strain at max. stress	*G* modulus at origin (MPa)	*E* modulus at origin (MPa)
Average shear (0 °C)						
1	8144.37	1.118	21.718	1.118	313.402	940.206
2.5	6766.00	1.139	18.043	0.456	736.713	2210.139
Average shear (20 °C)						
1	4306.79	0.958	11.485	0.958	227.418	682.254
2.5	4358.92	1.510	11.624	0.604	587.462	1762.387
Average shear (60 °C)						
1	785.82	0.590	2.096	0.590	3.628	10.885
2.5	319.16	1.172	0.851	0.469	1.818	5.455

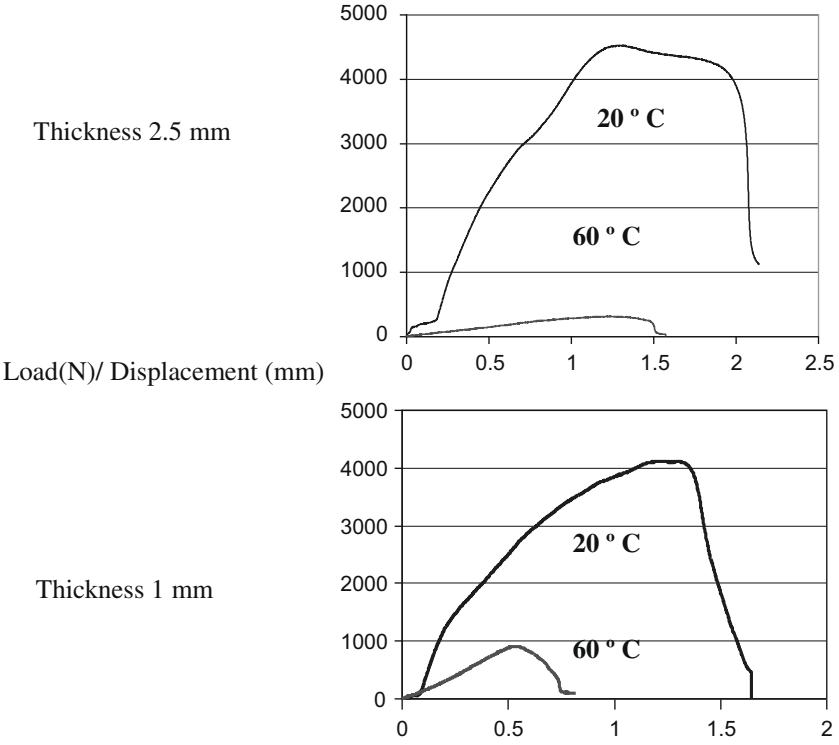

Fig. 9. Shear test results at different temperature and adhesive layer thickness.

levels of load were checked (5000 N and 10,000 N) corresponding approximately with 30% and 60% of the maximum static load. A minimum load of 500 N was maintained in order to avoid the total unload of the specimen while the test was performed. Three sinusoidal frequencies of load were used to simulate the effect of dynamic actions such as wind or seismic forces (Table 3).

Table 3 summarizes the results of the dynamic tests. It was observed that the more the amount of adhesive, the larger the area enclosed in the load–displacement graphic. It corresponded to the energy dissipated per cycle. In order to obtain a comparison value, the energy dissipated per cycle was divided by the volume of the adhesive layers of each specimen.

Fig. 13 plots the results of three dynamic tests with different frequencies. It can be observed that the higher the frequency the narrower the hysteretic loop.

5. Discussion of results

The behaviour of the toughened epoxy resin under the standard shear test (fracture mode II) showed a decrease of the stiffness and, therefore, of the shear modulus, as the load increased. It can be considered elastic at the origin and plastic in a following stage.

The material was thermal-sensitive as the shear average strength at 0 °C was 20 MPa, at 20 °C was 10 MPa and at 60 °C

Table 2
Cleavage standard test results.

Cleavage tests thickness (mm) and temperature	Adhesive thickness (mm)	Load (N)	Displacement (mm)	Average cleavage stress (MPa)	Max. tension stress (MPa)
Aver cleavage (0 °C)					
0.5	0.5	4835.76	0.807	7.74	30.95
1	1	4561.11	0.924	7.30	29.19
1.5	1.5	4308.06	0.937	6.89	27.57
2.5	2.5	3807.07	0.991	6.09	24.37
Aver cleavage (20 °C)					
0.5	0.5	3598.3	0.797	5.757	23.029
1	1	3271.0	0.858	5.234	20.934
1.5	1.5	2948.4	0.839	4.717	18.870
2.5	2.5	3059.2	0.869	4.895	19.579
Aver cleavage (40 °C)					
0.5	0.5	1237.87	0.579	1.98	7.92
1	1	886.917	0.559	1.42	5.68
1.5	1.5	720.978	0.7349	1.15	4.61
2.5	2.5	679.016	0.8012	1.09	4.35
Aver cleavage (60 °C)					
0.5	0.5	629.45	0.4157	1.01	4.03
1	1	587.46	0.4536	0.94	3.76
1.5	1.5	442.5	0.4697	0.71	2.83
2.5	2.5	320.43	0.4512	0.51	2.05

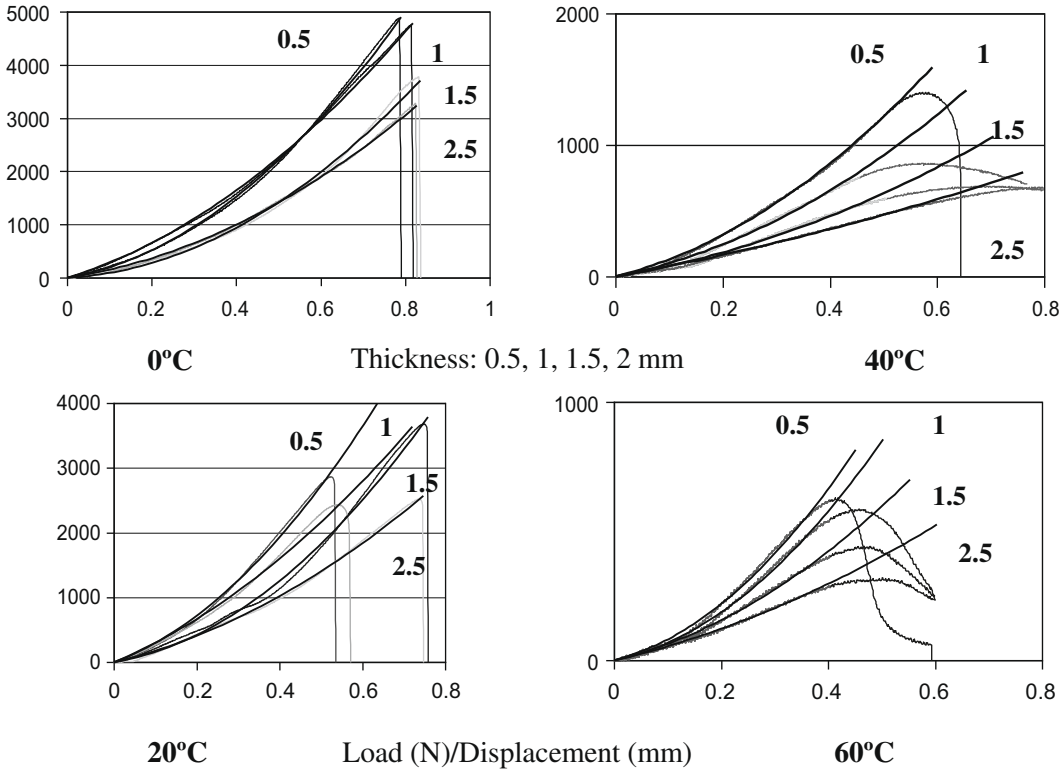

Fig. 10. Cleavage test results at different temperature and adhesive layer thickness.

Table 3
Dynamic bending test results on non-standard specimens and different thicknesses.

V-joint (adhesive thickness)	Frequency (Hz)	Load (N)	A_{max} (E_{abs}) (kN mm)	A_{min} (E_{dev}) (kN mm)	A_{int} (E_{disip}) (kN mm)	$A_{int/volume}$ (kN mm/mm^2)	Damping (%) (E_{disip}/E_{abs})
2.5 mm symmetric	0.5	5000	0.4288	0.3438	0.0850	0.0002655	19.82
		10,000	1.0080	0.7692	0.2388	0.0007459	23.69
	1	5000	0.3292	0.2808	0.0484	0.0001512	14.70
		10,000	1.0650	0.8635	0.2015	0.0006294	18.92
	2	5000	0.3609	0.3197	0.0412	0.0001287	11.42
		10,000	1.0730	0.9377	0.1353	0.0004226	12.61
2.5–0.5 mm asymmetric	0.5	5000	0.3429	0.2681	0.0748	0.0003894	21.81
		10,000	1.0970	0.9285	0.1685	0.0008772	15.36
	1	5000	0.3692	0.3001	0.0691	0.0003597	18.72
		10,000	1.0746	0.9673	0.1073	0.0005586	9.99
	2	5000	0.3490	0.2827	0.0663	0.0003451	19.00
		10,000	1.1705	1.064	0.1065	0.0005544	9.10
0.5 mm symmetric	0.5	5000	0.3364	0.2999	0.0365	0.0005700	10.85
		10,000	1.0594	0.8988	0.1606	0.0025082	15.16
	1	5000	0.3476	0.3134	0.0342	0.0005341	9.84
		10,000	1.1440	1.0045	0.1395	0.0021786	12.19
	2	5000	0.3419	0.3004	0.0415	0.0006481	12.14
		10,000	1.0040	0.9322	0.0718	0.0011213	7.15

was around 1–2 MPa, depending on the thickness. This fact accords with the behaviour observed by Tadeu and Branco [11,12]. The thickness increase produced a slight decrease of strength, although the plastic stage grown.

The cleavage standard test results (fracture mode I) showed an increase of the stiffness and, therefore, of the Young modulus, as the load increases. The influence of the temperature in the standard cleavage test results followed the same pattern as the shear test, although with a lower effect.

It can be highlighted that the increase of the thickness did not mean an increase of the displacement at failure. It occurred because the difference of stiffness between the adhesive and the adherends produced shear stresses at the adhesive layer near the contact surface. It must be considered that cleavage mainly results from a combination of tensile loads and bending moment [20].

In the three points static bending test results, the linear behaviour of the graphic "load versus load-head-displacement" appeared to be a useful element to performance numerical models of the new V-joint configuration.

"Load versus lateral displacement" graphics point out that there was a combination of cleavage and shear stresses under transversal loads. The failure happened due to cleavage stress, because in the

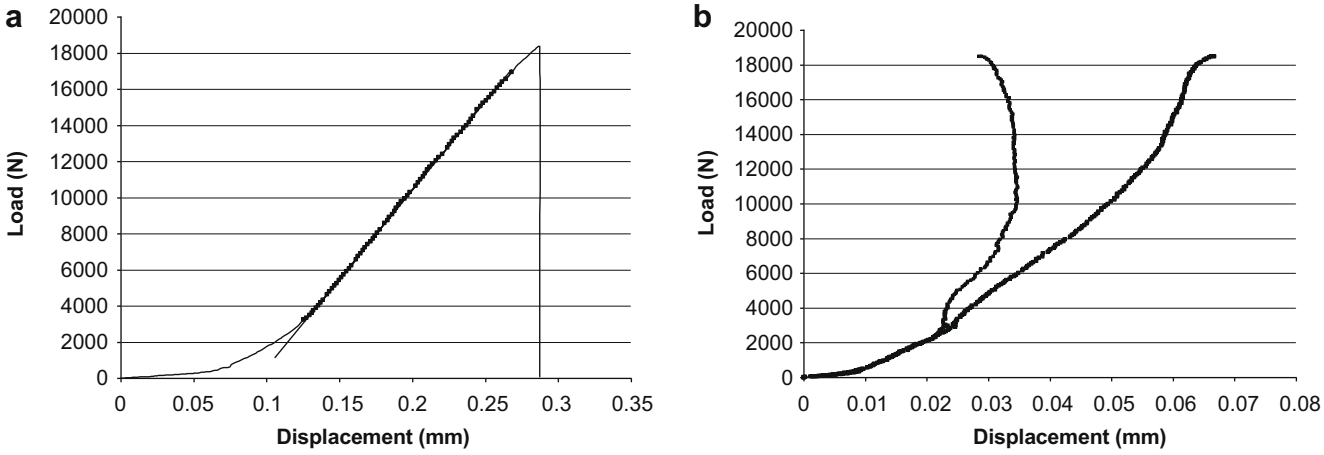

Fig. 11. Static bending tests. Load versus load-head-displacement curve (a) and lateral-displacements curves (b).

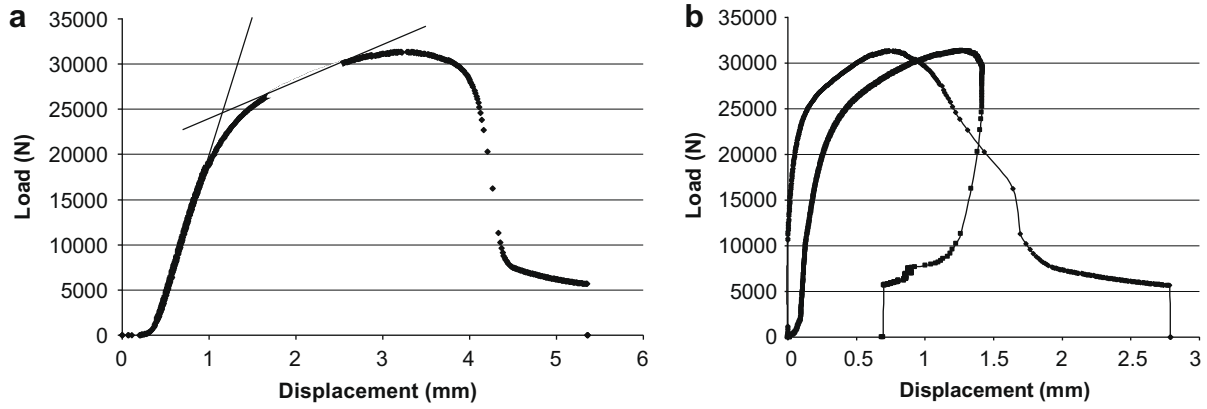

Fig. 12. Static compression tests. Load versus load-head-displacement curve (a) and load versus lateral-displacements curves (b).

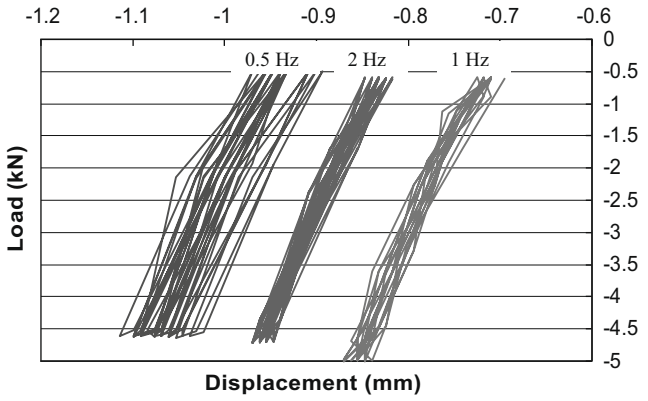

Fig. 13. Dynamic bending test; load versus displacements under different frequencies (0.5, 1 and 2 Hz).

side where the failure occurred, the graphic fit with the parabolic behaviour recorded in the standard cleavage tests. This feature can be used as a reference value in order to build up a FEM numerical model, for its use with other materials in this joint design.

In the graphics obtained from the static compression tests, it can be observed a combination of two models of behaviour: compression and shear. Compression was the main stress in the first stage of load, coincident with a linear pattern and no lateral displacements. That confirmed it was compression.

In the second stage of load, the graphic was linear too, but with a decrease of the stiffness. As lateral displacements of the joint piece occurred, the hypothesis of shear stress was confirmed. The increase of lateral displacements implied a permanent deformation in the joint material and, therefore, permanent damage.

The energy dissipation capacity, represented by the enclosed area between the load and unload stages of the curve "load versus displacement" on the dynamic bending tests, indicated that the material used in the configuration produced a damping effect. The displacement of the peaks of the graphic implied that there was some permanent deformation in the joint material (creep).

6. Summary and conclusions

A new bonded vertical joint for steel architectural panels is presented which can overcome the disadvantages of conventional straight joints. The constructive and aesthetic advantages, in addition to its improved mechanical behaviour, make this new solution a good alternative for conventional vertical joint.

The static and dynamic tests carried out on the vertical joint half scale specimens, with the inclusion of a V-shaped piece, showed a satisfactory behaviour due to its mechanical collaboration. The new configuration increases the joint toughness and makes it more durable because, according with fracture mechanics theory, the cracks or defects which coalesce in cracks have to propagate by mixed mode, cleavage and shear (modes I and II respectively, instead of cleavage only (mode I).

The use of a toughened epoxy resin as joint material in this new joint design gives a viscoelastic damping capacity to the façade under dynamic forces. The behaviour showed by the selected toughened epoxy at room temperature was excellent, though it showed worse performance under moderate conditions of temperature. Therefore, another toughened epoxy resin, with a better temperature performance, must be considered.

The combination of standard and non-standard tests on scale specimens would allow the development and adjustment of finite elements models in order to simulate joint performance under different external loads. Further research is also needed in order to evaluate durability issues concerning the joint material.

Acknowledgements

The authors acknowledge with thanks the Polytechnic University of Madrid for the scholarship given to Gonzalo Barluenga and the Glasgow Marine Technology Centre for all the human and technical support supplied for the experimental research. They also want to acknowledge the valuable comments of the reviewers which has undoubtedly improve the quality of this paper.

References

[1] Harriman MS. Breaking the mold. Architecture 1991;80:77–83.
[2] Martin B. Construcción, las juntas en los edificios. Barcelona: Gustavo Gili; 1981 [in Spanish from Martin B. Joints in buildings, Wiley 1977 in English].
[3] Arnold C. Cladding design: recent architectural trends and their impact on seismic design. In: Proceedings of the architectural precast concrete cladding. Chicago (IL): PCI; 1989. p. 14–31.
[4] Barluenga G. The joint in building systems of elements for façade: constructive, aesthetic and structural functions. Ph.D. thesis, Department of Building and Building Technology, School of Architecture, Polytechnic University of Madrid; 2002. (in Spanish).
[5] Barluenga G, Hernández-Olivares F, Leon RT. Seismic response of a new design for vertical joints in architectural panels. Eng Struct 2003;25:1655–64.
[6] Barluenga G, Hernández-Olivares F. SBR latex modified mortar rheology and mechanical behaviour. Cem Concr Res 2004;34:527–35.
[7] Knox EM, Cowling MJ, Winkle IE. Adhesively bonded steel corrugated core sandwich construction for marine applications. Mar Struct 1998;11:185–204.
[8] Hashim SA. Adhesive bonding of thick steel adherends for marine structures. Mar Struct 1999;12:405–23.
[9] Knox EM, Cowling MJ, Hashim SA. Creep analysis of adhesively bonded connections in GRE pipes including the effect of defects. Composites Part A 2000;31:583–90.
[10] Kinloch AJ. Adhesion and adhesives. London: Chapman & Hall; 1987.
[11] Tadeu A, Branco F. Shear tests of steel plates epoxy-bonded to concrete under temperature. J Mater Civ Eng 2000;12:74–80.
[12] Branco F, Tadeu A, Nogueira J. Bond geometry and shear strength of steel plates bonded to concrete on heating. J Mater Civ Eng 2003;15:586–93.
[13] Aiello MA, Frigione M, Acierno D. Effects of environmental conditions on performance of polymeric adhesives for restoration of concrete structures. J Mater Civ Eng 2002;14:185–9.
[14] Frigione M, Lettieri M, Mecchi AM. Environmental effects on epoxy adhesives employed for restoration of historical buildings. J Mater Civ Eng 2006;18:715–22.
[15] Permabond™ E04. Two parts epoxy resin. Technical information sheet.
[16] Chikhi N, Fellahi S, Bakar M. Modification of epoxy resin using reactive liquid (ATBN) rubber. Eur Poly J 2002;38:251–64.
[17] Russell B, Chartoff R. The influence of cure conditions on the morphology and phase distribution in a rubber-modified epoxy resin using scanning electron microscopy and atomic force microscopy. Polymer 2005;46:785–98.
[18] Stewart I, Chambers A, Gordon T. The cohesive mechanical properties of a toughened epoxy adhesive as a function of cure level. Int J Adhes Adhes 2007;27:277–87.
[19] Ivanova KI, Pethrick RA, Affrossman S. Investigation of hydrothermal ageing of a filled rubber toughened epoxy resin using dynamic mechanical thermal analysis and dielectric spectroscopy. Polymer 2000;41:6787–96.
[20] Odette GR, Yamamoto T, Rathbun HJ, He MY, Hribernik ML, Rensman JW. Cleavage fracture and irradiation embrittlement of fusion reactor alloys: mechanisms, multiscale models, toughness measurements and implications to structural integrity assessment. J Nucl Mater 2003;323:313–40.